TRIBOLOGICAL PROPERTIES OF IONIC LIQUIDS LUBRICANTS CONTAINING NANOPARTICLES

A Thesis

by

WEI LU

Submitted to the Office of Graduate and Professional Studies of
Texas A&M University
in partial fulfillment of the requirements for the degree of

MASTER OF SCIENCE

Chair of Committee,	Mustafa Akbulut
Committee Members,	Tahir Cagin
	Hong Liang
Head of Department,	M. Nazmul Karim

May 2014

Major Subject: Chemical Engineering

ABSTRACT

Recently, there has been an increase in research in the application of ionic liquids containing nanoparticles as lubricants due to their properties such as thermally stability, non-volatility and non-flammability. The purpose of this thesis is to describe the tribological and rheological properties of mixtures of nanoparticles (NPs) and ionic liquids (ILs), specifically the mixture of bare SiO_2 (silica) nanoparticles and ionic liquid 1-butyl-3-methylimidazolium (trifluoromethysulfony)imide and the mixture of SiO_2 nanoparticles functionalized by octadecyltrichlorosilane (OTS) and ionic liquid1-butyl-3-methylimidazolium (trifluoromethysulfony)imide. Functionalized SiO_2 nanoparticles dispersion in ionic liquid was compared to that of the bare SiO_2 nanoparticles, and shown that functionalized SiO_2 nanoparticles led to improved colloidal stability. Friction force profiles, friction coefficients, viscosity behavior, wear behavior of these mixtures at various nanoparticles concentrations for a tribo-pair of stainless steel ball and a steel surface were also investigated. It was shown that the friction coefficient of the OTS functionalized SiO_2 nanoparticles for the optimum concentration (0.1 wt.%) was 36% less than that of the pure ionic liquid, while the friction coefficient of the bare SiO_2 nanoparticles and the ionic liquid mixture at the optimum concentration (0.05 wt.%) was 23% less than that for the pure ionic liquid. Moreover, friction surfaces of the two kinds of silica nanoparticles at the optimum concentration were examined by scanning electron microscopy (SEM) and friction traces. Eventually, it has been shown that promising tribological properties of ionic liquids can be further enhanced by incorporating bare SiO_2 nanoparticles into ionic liquids. Moreover, the tribological

performance of the mixture of the OTS functionalized SiO_2 nanoparticles and ionic liquid could be better than that of the mixture of bare SiO_2 nanoparticles in the same ionic liquid.

DEDICATION

This thesis is dedicated to my parents and husband, for their unconditional love and support throughout the course of my academic career.

ACKNOWLEDGMENTS

I would like to thank my advisor, Dr. Mustafa Akbulut, for all his research guidance, for his confidence in my ability. Without his support and help, I would never have been exposed to field of scientific research. I would like to thank Dr. Sreeram Vaddiraju, Dr. Sue, Hung-Jue and Dr. Victor Ugaz for letting me use the FT-IR100 spectrometer, the thermal gravimetric analysis (TGA) equipment and rheological measurements equipment in their labs. I would like to thank my colleagues: Kheireddin, Bassem Ali, Chen, I-Cheng, Yegin, Cengiz and Zhang, Ming for their instruction and help to finish my experiments. I would like to thank my friend, Yidong Pan for teaching me to do FT-IR analysis. I really appreciate all your time spent educating me and sharpening my skills as an engineer and researcher.

TABLE OF CONTENTS

Page

LIST OF FIGURES

Page

Page

1. INTRODUCTION

The purpose of this thesis is to present the results of a yearlong research project on tribological properties of two kinds of lubricants: one is ionic liquid lubricant (1-butyl-3-methylimidazolium (trifluoromethysulfony)imide) containing the bare SiO_2 nanoparticles, another is the same ionic liquid lubricant containing SiO_2 nanoparticles functionalized by octadecyltrichlorosilane (OTS). There are four sections in this thesis. Section 1 begins with a brief overview of fluid lubrication, an introduction of the application and development of pure ionic liquids as lubricants and a literature review of the application of nanoparticles in fluid lubricants. Section 2 describes experimental techniques and methods used in this study. In this section, the methods and characterization used in this study include Fourier Transform Infrared Spectroscopy (FTIR), thermal gravimetric analyses (TGA), nanotribometer, rheological measurements, dynamic light scattering (DLS). At the same time, the information on the materials and procedures used in this research project is given. Section 3 consists of the experimental results and discussion. Section 4 summarizes and concludes the thesis.

1.1 Fluid lubrication

1.1.1 Tribology

The word “tribology” is derived from Greek word “tribos”, which means “rubbing”. Nowadays, in the study of friction and lubrication engineering, tribology is defined as the science and technology of interacting surfaces in relative motion and of related subjects and practice [1]. The definition of tribology integrates individual technology into engineering related to friction, so tribology generates interdisciplinary

fields ranging from fundamental research to industrial applications such as nanotechnology and surface sciences. From an economic viewpoint, the study of tribology in practice is important, UK scientist H. Peter Jost estimated in his famous "Jost Report" to British government that the appropriate application of tribological principles and practices in industry can result in the savings of 1.0% to 1.4% of a country' gross national product (GNP) [2].

1.1.2 A brief history of oil lubricants

The use of lubricating oils can be traced back to ancient Egypt. At that time, people have been aware that certain liquids between surfaces in relative motion could reduce friction [3]. In the middle of the 19th century, with the discovery of petroleum, the petroleum-based lubricants, also called mineral oils, have been used and developed for various machines after the Industrial Revolution. However, with the development of rocket motors and space vehicles, as well as the discovery of the gas turbine in World War II, people found that at condition of extreme temperature, mineral oil lubricants were not suitable for applications in the harsh condition. For example, mineral oil lubricants were easy to oxidize at temperatures above 100°C and it would become very viscous or gelatinous at temperatures below -20°C. Because of the disadvantages of mineral oil lubricants, synthetic lubricants and lubrication additives intended for extreme conditions, such as higher loads, extreme temperature and vacuum, became also available. The most common examples of synthetic lubricants are silicone oils, the PFPE lubricant, PAOs and polyesters. These synthetic lubricants have been extended to the useful range of fluid-film lubrication from temperature of -70°C to 300°C [4].

1.1.3 Fluid lubrication mechanisms and types

In practice, various kinds of devices and machines need lubricants for sliding pairs. Lubricants can be divided into three kinds: fluid lubricants such as water or mineral oils, greases, and solid lubricants (self-lubricating materials) such as graphite. In the three categories, fluid lubricants are most commonly used in practices. Fluid lubricants have a series of advantages compared to greases and solid lubricants, such as long term endurance, low mechanical noise, promotion of thermal conductance and very low friction in the elastohydrodynamic regime [5].

When a viscous fluid lubricant is introduced between two motion friction surfaces, the two sliding surfaces are separated by this fluid lubricant, so that friction and wear between the two motion surfaces are reduced. According to the separation distance, the lubricants can be divided into three regimes which are shown in the well-known Stribeck curve [6] as illustrated in Figure 1. Regime (1) is the regime for hydrodynamic lubrication. In this regime, the viscous liquid is introduced between the surfaces and a stable liquid film is formed. The applied load is completely supported by the liquid film and the two surfaces never come into direct contact so that the friction is reduced between the friction surfaces. Moreover, in this regime, the lubricant performances are decided by the viscosity of the lubricant, applied loads to the contact and sliding velocity. Regime (2) is the elastohydrodynamic lubrication (EHL) regime. In this regime, the thickness of the lubrication liquid film is obviously much lower than that found in hydrodynamic lubrication. The asperities on the two surfaces can have chance to contact, in which case elastic deformation will occur and the loads will be dispersed

by the viscous resistance of oil. Regime (3) is the boundary lubrication regime. In this regime, the lubrication liquid film breaks down and the asperities come into closer contact causing ‘‘stick–slip’’ and break-off of some asperities, when the lubrication liquid film is thinner than elastohydrodynamic lubrication. Friction and wear under this condition are more severe.

In the hydrodynamic and EHL regimes, when the fluid viscosity and sliding speed are high enough or the load is low enough, the lubrication friction coefficient is proportional to the viscosity or viscosity pressure coefficient of lubricating oil. In boundary lubrication, the lubrication performance is determined by the film formation. When the viscosity of lubricant and sliding speed are very low, or the load is high, liquids are substantially suppressed and form a solid-like adsorption film at contact points, which is capable of supporting load and prevents serious breakdown. Direct contact between two surfaces leads to wear of the materials. During the process of friction, friction heat is generated under this condition so that reactions called tribochemical reactions or mechanochemical reactions are activated to form a tenacious film on the friction. This film also helps to prevent direct contact and severe wear of the friction surfaces.

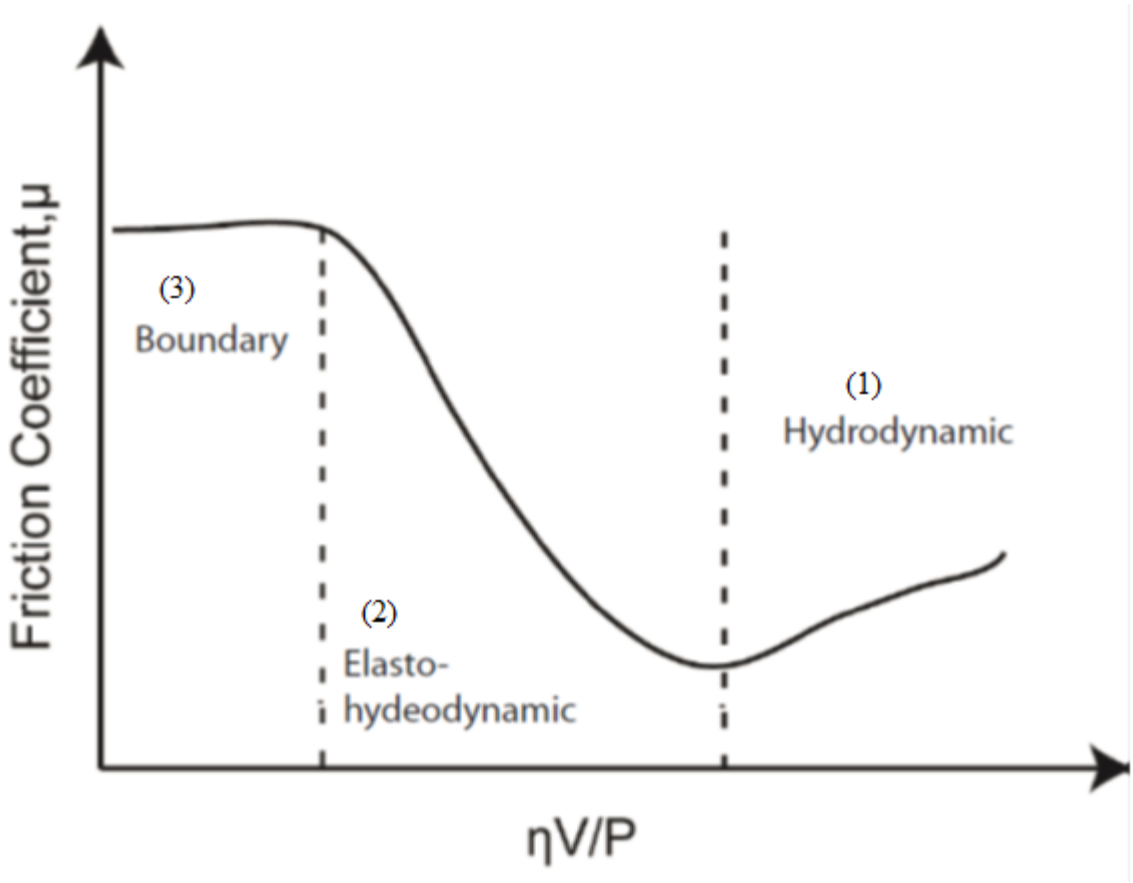

Figure 1. Fluid lubrication regimes illustrated by Stribeck curve. Where μ is the fiction coefficient, η is the dynamic viscosity of the lubricant, V is the sliding velocity and P is the applied load.

1.2 Overview of ionic liquids

1.2.1 Definition, types and properties of ionic liquid

Ionic liquids are defined as salts with melting points lower than 100°C. When their present melting points are lower than room temperature, they are called room-temperature ionic liquids. Ionic liquids are usually composed of an organic cation

containing nitrogen or phosphorus, and a weakly coordinating anion. Some of the most common cations are shown in Figure 2. They include imizaolium, phosphonium, pyridinium and ammonium. Some of the most common anions include BF_4^-, PF_6^-, $CF_3SO_3^-$and $N(CF_3SO_2)_2^-$ [7]. According to the property of anions, ionic liquids can be categorized into hydrophobic ionic liquids with weak hydration capacity, and hydrophilic ionic liquids.

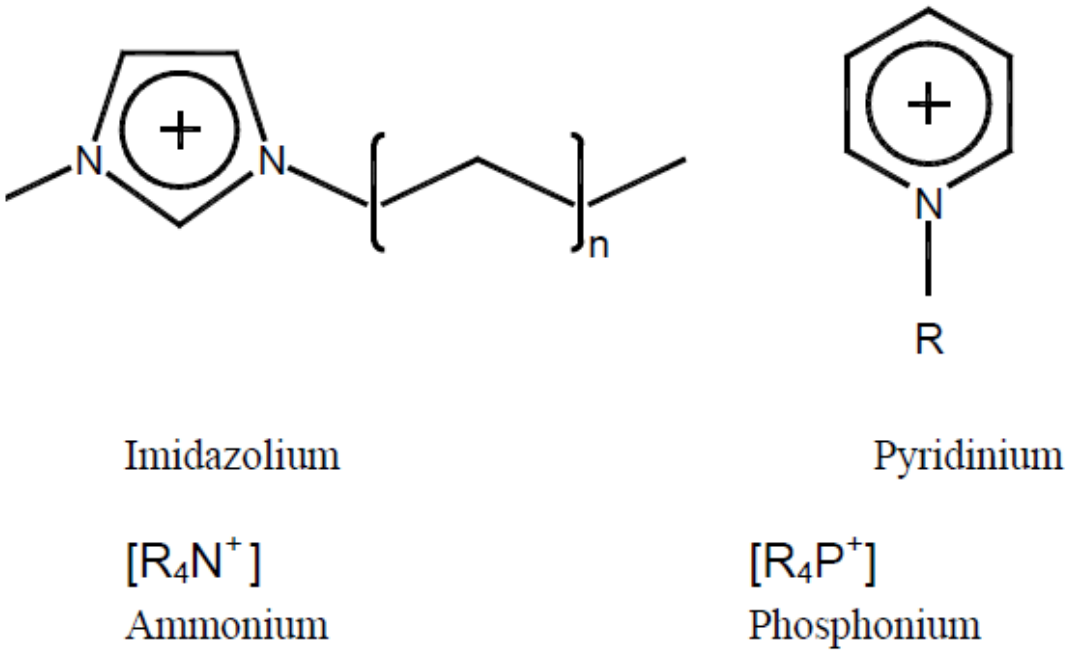

Figure 2. Some common IL cations used in lubrication and surface modification.

The melting point and the viscosity of ionic liquids are determined by the molecular structures, the types of cations and the length of alkyl chains[8]. Liu and coworkers [3] have summarized a series of properties of ionic liquids according the types and natures of anions and cations as following: (1) if the anion and alkyl chain on cation are the same in ionic liquids, the viscosities increase in the order imidazolium <pyridinium < pyrrolidinium; (2) for imidazolium ionic liquids, with the increasing alkyl chain length starting from methyl, the melting points decrease at first due to the reduced polarity, and then the melting points begin to increase when the carbon number is above 5 because of increased packing orders; (3) the viscosity of ionic liquids increase and the viscosity index decreases with the increasing of longer alkyl chains in imidazolium cations; (4) the viscosity increases with anion types following the trend of Tf_2N^- < FAP^- < $BETI^-$ < BF_4^- <PF_6^- < Cl^- < Br^-. Moreover, ionic liquids possess high viscosity because their highly structural symmetry. Besides high viscosity, ionic liquids also have other unique physical and chemical properties such as negligible volatility, high polarity, high thermal stability, nonflammability, miscibility with water and with organic solvents and electrochemical properties [7]. Because of these properties ionic liquids become a new green solvent or lubricant in industrial application.

1.2.2 The application of ionic liquid in tribology

1.2.2.1 Ionic liquids as lubrication oils

Many unique characteristics of ionic liquids have met the high performance requirement for lubricants. Particularly their high polarity can result in formation of a very strong and effective adsorption film and tribochemical reaction which contributes to

enhanced anti-wear capability. So ionic liquids can be used as a unique type of lubrication liquid. Ionic liquids upon the 1-n-alkyl-3-methylimidazolium cation were first reported in 1982 by Wilkes et al.[9] In 1992, Wiles and Zaworotko [10] found an air and water stable ionic liquid based on the tetrafluoroborate anion which was the first ionic liquid as lubricant. From 2001, Liu et al. [11] started to develop a series of researches in the field of ionic liquids lubrication. In their studies, alkyl-imidazolium tetrafluoroborate in steel/steel, steel/aluminium, steel/copper, steel/SiO2, steel/Si(100), steel/sialon and Si_3N_4/sialon ceramic contacts shows excellent friction reduction and has a low friction coefficient as compared to other synthetic oil such as PFPE and X-1P.

Ionic liquids have pure points (the lowest temperature to keep flow at 45° tilting angle) below -50°C, and their decomposition temperature can be up to 400°C. These properties of ionic liquids make it possible for them to keep good tribology properties in a wide temperature range. For example [12], the ionic liquid [C2C6im]BF_4 could lubricant steel/steel contact above 600N at 100°C in a ball-on-disc test, while maximum loads for X-1P and PFPE under the same conditions are only 300N.

Ionic liquids can be applicable as lubrication under vacuum because of their low volatility. Suzuki, A. et al investigated tribological characteristics of two imidazolium-based ionic liquids, 1-hexyl-3-methylimidazolium hexafluorophosphate ([HMIM]PF6), and 1-hecyl-3-methylimidazolium tetrafluoroborate ([HMIM]BF4) under high vacuum conditions [13]. They found that Imidazolium-based ionic liquids have relatively good viscosity-temperature characteristics, high thermal stability and low vapor pressure. Due

to these characteristics, ionic liquids show low friction and low wear rate under high vacuum conditions, and high load-carrying capacity.

For alkylimidazolium ionic liquids, their viscosity and tribological properties can be changed due to the alkyl chain length. In EHL regime, the viscosity of ionic liquids increase with the increase of alkyl chain length, therefore the ionic liquids have the better tribological performance. Moreover, besides the effect of alkyl chain length to tribological properties, the anions in ionic liquids also play an important role because they can change the viscosity and form the boundary film including physical adsorption and chemical reaction film. The reaction of anions contacting with the surface results in complicated tribochemical reactions during friction, therefore, compared to lubricants without these types of anions ionic liquids have the superior tribological characteristics.

1.2.2.2 Ionic liquids as lubricant additives

Because ionic liquids have better tribological performance, stronger boundary film formation capability, and lower cost than normal additives, they can have a high performance-to-price ratio. So the use of ionic liquids as additives in water, mineral oils or synthetic oils is a feasible and economic choice.

Phillips et al. [14, 15] investigated the use of ionic liquids as additives in water. The results showed that when ionic liquids are used as additives in water, they can reduce the running-in period (the initial period of high friction) of ceramic-ceramic sliding contacts. In their researches, BFx and PFx films were formed on the surface and an electric double layer of ionic liquids molecules was generated during the process of

initial mechanical wear, therefore the local viscosity near the surface and the load carrying ability increased, and the friction and wear decreased.

Bermudez et al. [16] have studied the application of ionic liquids as additives in mineral oil. They used 1wt% 1-n-Alkyl-3-methylimidazolium ionic liquids in a paraffinic-naftenic mineral base oil for SAE 52100 steel and ASTM 2011 aluminum contacts at room temperature and at 100°C. Their research results indicated that when sliding velocities were relatively high, both lubrication and anti-wear properties were better than those in pure ionic liquids tests. These pure ionic liquids have different side chain lengths on the cations, therefore for the same anion [BF_4^-], ionic liquids containing cations with longer alkyl chains are more effective in the use as lubrication, for example, octyl-([$OMIM^+$]) > hexyl-([$HMIM^+$] > ethyl-([$EMIM^+$]). However, when ionic liquids are used for additive, those containing cations with shorter alkyl chains are more effective, for example, [$EMIM^+$] > [$HMIM^+$] > [$OMIM^+$].

Bermudez et al. also studied the application of ionic liquids as additives in synthetic oils. They used 1wt% 1-n-Alkyl-3-methylimidazolium ionic liquids in the synthetic ester propylene glycol diolete for SAE 52100 steel and ASTM 2011 aluminum contacts at room temperature and at 100°C [17]. In the research, the synthetic oils with ionic liquids additives can reduce friction and wear compared to identical tests using the base oil without ionic liquids additives. Yao, M. et al. [18] evaluated the performance of dicationic bis(imidazolium) ionic liquids as additives in polyethylene glycol for steel-steel sliding pairs at room temperature. These ionic liquids contain the same long side-

chain substituted cations and different anions. Results showed that they could effectively reduce the friction and wear compared to the base oil without additives.

1.2.3 Lubrication mechanisms of ionic liquids as lubricants

To better understand the mechanism of ionic liquid's behaviors as lubricants or lubricant additives, many researchers studied the reaction of ionic liquids with solid surfaces, and characterization of the boundary layer that forms in the process of lubrication.

Most theories currently accepted by researchers put emphasis on the film formation capability and its interaction strength with the sliding surface, since elasto-hydeodynamic and boundary lubrication decide the tribological performance. For example, some researchers have found that ionic liquids based on PF_6^- and BF_4^- anions lead to significant improvements in wear performance for silicon and aluminum surfaces. Forsyth et al. [19] have studied the ionic liquids lubrication mechanisms and proposed the basic adsorption models. When the sliding surfaces are metals or ceramics, the nature of the boundary layer depends on the substrate surfaces. For example, for the surface of ionic liquid-lubricated steel/iron surfaces in extreme temperature, some iron samples were oxidized to Fe_2O_3 and Fe_3O_4 before the ionic liquids were introduced between the surfaces. The Fe_2O_3 and Fe_3O_4 interact strongly with ionic liquid anions and cations. The anions in ionic liquids bond to the surface, and subsequent cations are attracted to this layer, forming an electrical double layer. Carper et al. [20] proposed an adsorption model based on a semi-empirical thermodynamic method. The interactions between ionic liquids and either metal or ceramic surfaces (the enthalpies) can determine

the tribological properties. The measured frictional coefficients are inversely proportional to the enthalpies, consistent with the concept that the stronger interacting ionic liquids provide better lubrication capability.

Kajdas [21] further developed the anion multilayered adsorption model. In the model, the author proposed that the friction between sliding surfaces led to the release of low energy electrons from contact convex point on the sliding surfaces. At the same time, positive charges formed at the surface of convex due to the release of low energy electrons. This mechanism strengthens the adsorption mode. When ionic liquids were introduced into the sliding surface, the anions in ionic liquids can adsorb onto these positively charged sites, and the counter cations assemble successively according to the electroneutrality principle. Therefore, ionic liquids' structural arrangement is a multilayered adsorption under medium-high pressure, rather than a single-layer adsorption on sliding surfaces. This multilayered structure contributes to the good lubricity of ionic liquids. Moreover, the length of alkyl chain of ionic liquids has effect on the tribological properties of ionic liquids because of the multilayered adsorption phenomenon. Formation of the multilayer adsorption films leads to more enthalpy being obtained during the process, therefore the ionic liquids with longer alkyl chains are easier to form a densely packed structure with much better tribological properties.

1.3 Nanoparticle-based lubrication systems

Generally, three kinds of additives are often used in lubrication systems [22]:

(1) Organic compounds such as zinc dialkyl dithiophosphate (ZDDP), tricresyl phosphate (TCP), trixylyl phosphate (TXP) and dilauryl phosphate, etc.

(2) Particulate solid lubricants such as MoS_2 and graphite, etc.

(3) Nanoparticles.

Organic compounds are limited in their use because of related environmental problems. This kind of additives has corrosion effects to metal specimen and their manufacturing and use may cause pollution to environment. Particulate solid lubricants have poor solubility and low dispersibility in lubricating oils. These shortcomings limit their further application as additives in formulated lubricants. Since the physical and chemical properties of nanoparticles are quite different from those of the other additives, application of nanoparticles have been extensively studied in many areas, especially in the field of tribology. Recent research has shown that Nanoparticle-Based Lubrication Systems (NBLS) has improved lubrication properties compared to systems with traditional lubricant additives [23-29]. It is anticipated that nanoparticle additives may integrate the advantages of organic compound additives and solid lubricant additives.

1.3.1 Mechanism of lubrication with nanoparticles

Numerous nanoparticles used as oil additive have been investigated in recent years. Results show that nanoparticles deposit on the rubbing surface and improve the tribological properties of the base oil, and display good friction and wear reduction characteristics even at concentrations below 2%wt. [30]. Over the past few decades, researchers have tried to explain the reasons behind the improved lubricity through various mechanisms. Most researches show that the reason for lubricity improvement is the increase of the load carrying capacity due to the addition of nanoparticles in the base lubricant, therefore preventing the asperities from coming into intimate contact.

Peng summarized previous research work and specified four characteristics of anti-wear and friction reduction phenomena by nanoparticles added to base oil [31]. They are as follows:

(1) The nanoparticles are smaller than other conventional types of additives, so they are more likely to interact with the surfaces of the sliding to form a surface protective film.

(2) For spherical nanoparticles, they are more likely to roll between the surfaces; therefore, the sliding friction between two surfaces becomes the comnination of sliding friction and rolling friction.

(3) When there is an increase in the amount of nanoparticles which bear the compressive force dispersion, the compressive stress concentrations, which are related to high contact pressure, may be reduced.

(4) Nanoparticles can deposit on the sliding surfaces, and form a physical tribofilm which can make up the loss of mass of sliding surfaces. This effect is called the 'mending effect'. The combination of above effects provided the explanation on the good friction and wear properties of nanoparticles in lubrications.

Bessem [32] also reviewed previous mechanisms and divided them into three main categories according to the performance of nanoparticles: a) ball-bearing effect, b) smoothing out process, and c) tribofilm formation.

Firstly, considering the shape of nanoparticles, the mechanism is the ball-bearing effect when the nanoparticles are spherical or quasi-spherical in shape, as shown in Figure 3. When the load between rubbing surfaces is below a certain level, the shape and

rigidity of the nanoparticles have no change, which leads to these nanoparticles' size exceeding the surface roughness. These nanoparticles can roll between the sliding surfaces to decrease the friction and wear [33].

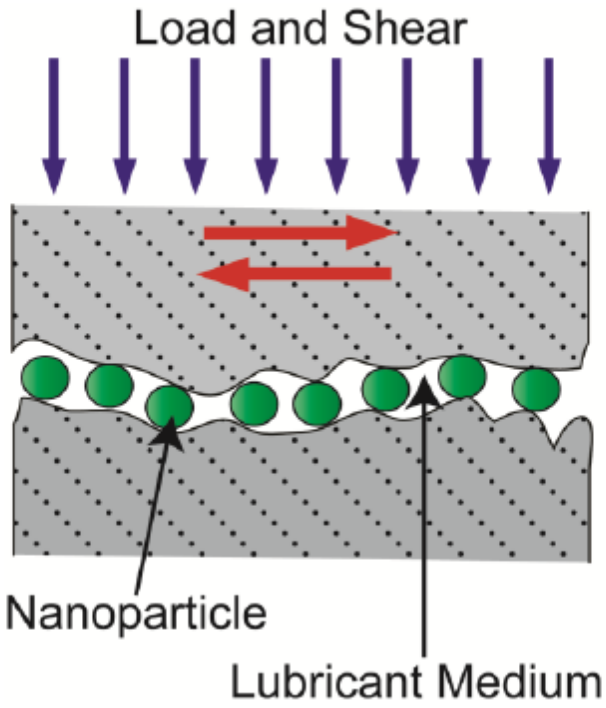

Figure 3. Illustration of the ball-bearing of mechanism.

Secondly, the smoothing out process is shown in Figure 4. It has been hypothesized and proven experimentally by researchers that nanoparticles could fill out

the valleys between the asperities on the rubbing surfaces. This results in the improvement of tribological properties because of the reduction of surface roughness.

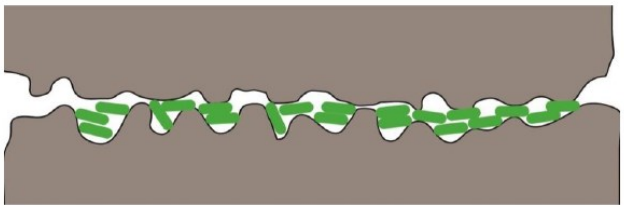

Figure 4. Schematic illustration of the artificial smoothing mechanism.

Thirdly, in the mechanism of tribofilm formation, there are certain physical or chemical interactions between the nanoparticles and the surfaces under boundary lubrication conditions during the sliding process. A protective tribofilm can be generated by nanoparticles depositing on the rubbing surfaces. Under these circumstances, the tribofilm can decrease the shearing stress since the nanoparticles can carry part of the load and prevent asperities from contacting each other, thereby exhibiting better friction and antiwear properties. Many researchers tried to explain the mechanism and composition of such tribofilm. In the research of Rapoport et al. [34], the tribological properties improved by adding IF-WS2 nanoparticles in lubricating oils, therefore they concluded that a physical protective film formed during the sliding process when

nanoparticles deformed then deposited on the interfaces. Liu et al. also summarized the anti-wear mechanisms of the nanoparticles additives [35, 36]. They reported that when the shearing is strong, nanoparticles may be melted and welded on the shearing surfaces, or reacted with specimen to form a protective layer, thus improving the anti-wear properties. Post friction surface characterizations have proved the existence of tribo-products of various kinds on wear scars, such as FeB and B_2O_3 on the rubbed surfaces, these tribo-products deposited on the surfaces to form a tribochemical film, the film can further prevent a fresh metal surface from serious wear. B. Li et al. proposed the anti-wear mechanism of the nanoparticulate additive could be depicted as follows. When ‘‘oil-soluble’’ nanoparticles were added into a lubricant, a homogeneous and stable colloid solution was formed.

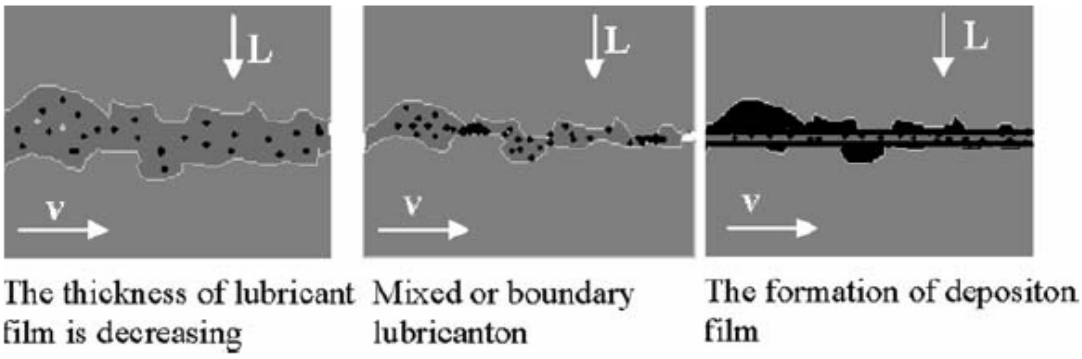

Figure 5. Schematic illustration of the mechanism of tribofilm formation mechanism for nanoparticles as lubricant additive.

When the lubricant film between tribo-pairs becomes thinner and mixed lubrication or boundary lubrication occurs, the nanoparticles (especially rigid nanoparticles such as TiO2) may carry a proportion of load and separate the two surfaces to prevent adhesion, thus benefit the anti-wear properties (Figure 5).

1.3.2 Colloidal stability

When common bare nanoparticles, such as metals, metal oxides, ceramic materials and chalcogenides, etc., are dispersed in inert non-polar liquids (such as hydrocarbons), the systems are often thermodynamically unstable and prone to aggregation. Their dispersive ability is very poor in organic solvents and based oils. This will ultimately lead to the precipitation of nanoparticles in oil. If the colloidal dispersion is poor, the lubricant with nanoparticle additives will not have a good enhancement effect on the tribological performance of the base oil. Bare nanoparticles usually experience material transfer when they come into direct contact with shearing surfaces. So in order to improve the effect of nanoparticles to lubricants, the main molecular forces between particles need to be studied. Generally, the main reason for nanoparticles aggregation is the Van der Waals forces which exist in these inter-particle interactions. Van der Waals forces are attractive forces in nature and generally favor the aggregation or flocculation of the particles. To better illustrate the Van der Waals forces, it is assumed that there are two spherical nanoparticles in a medium as depicted in Figure 6. They have the same radius R and the separation distance between them is D.

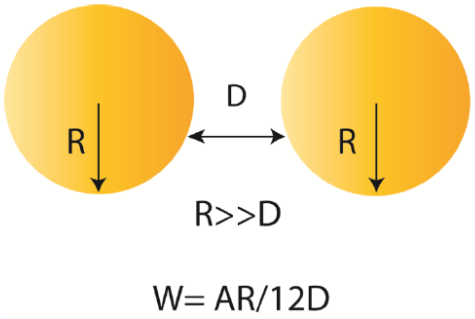

Figure 6. Schematic illustration of the interaction between two bare nanoparticles.

When their separation distance is very short (D << R), the energy of interaction W is given by equation (1):

$$W = -\frac{AR}{12D} \tag{1}$$

A is the Hamaker constant, which is typically in the order of 10^{-19} to 10^{-21} J. A is a function of properties of the suspended particle material and the suspending medium. A can be expressed by equation (2):

$$A = \frac{3}{4}kT\left(\frac{\varepsilon_1 - \varepsilon_3}{\varepsilon_1 + \varepsilon_3}\right)^2 + \frac{3h\nu_e}{16\sqrt{2}}\frac{(n_1^2 - n_3^2)^2}{(n_1^2 + n_3^2)^{\frac{3}{2}}} \tag{2}$$

k is Boltzmann's constant, T is the absolute temperature, ε is the dielectric constant (a measure of polarizability), h is Planck's constant, ν_e is the maximum electronic

absorbance frequency, and n is the refractive index. The subscripts 1 and 3 refer to the particle and medium, respectively.

The Hamaker constant is an important parameter since its sign determines whether the interaction is repulsive or attractive. When its sign is positive, the energy of interaction is negative and the interaction is attractive. Moreover, the Hamaker constant's magnitude determines the strength of the interaction.

Moreover, in order to solve the stability and dispersion problem of nanoparticles in base oils, it is also necessary to study the repulsions between nanoparticles, because the stability and suspension of nanoparticles in various media also depend on mutual repulsions between particles. In a typical suspension, the repulsive forces include electrostatic, steric, and solvation (structural) forces [38, 39], as illustrated in Figure 7.

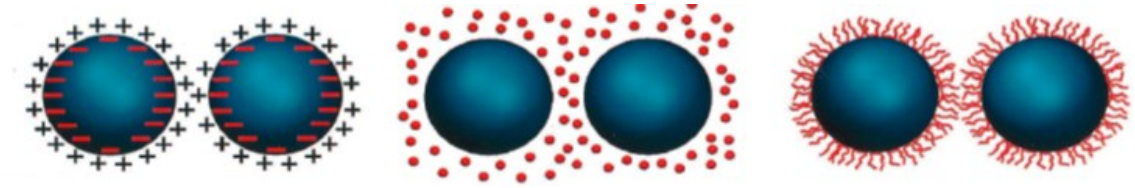

Figure 7. Schematic illustration of the interaction potential energy and relevant length scales for (A) electrostatic, (B) structural, and (C) steric contributions.

The electrostatic repulsion is a common repulsion used to stabilize nanoparticles in aqueous and organic media. The theory behind this type of interaction is based on the

fact that like-charged particles repel each other in accordance with Coulomb's law. In dilute systems, electrostatic repulsion complies with the classical Debye-Huckel theory. The magnitude and scale of electrostatic repulsion depend on the type of solvent (i.e. dielectric constant), concentration and chemical nature of the surrounding ions.

Another possible repulsion between particles is the solvation (structural) force. In the condition that liquid molecules are confined between two nanometer scale flat surfaces, ordered or layered structures are formed in the vicinity of a solid-liquid boundary. The structures can lead to a liquid density oscillation (So the solvation force is also called the oscillatory solvation force). The strength of the solvation force is decided by the ionic structure of ionic liquids, surface charge density, surface chemistry, surface roughness, and the amount of water [40].

Steric effects arise from the fact that each atom within a molecule occupies a certain amount of space. If atoms are too close to each other, there is an associated cost in energy due to overlapping electron clouds (Pauli or Born repulsion), and this may affect the molecule's preferred shape (conformation) and reactivity. Steric hindrance occurs when the large size of groups within a molecule prevents chemical reactions that are usually observed in related molecules with smaller groups.

Ueno reported the impact of these three different types of repulsions on the colloidal particle stability in ionic liquid medium [1]. When bare silica nanoparticles are dispersed in ionic liquids, ionic groups on the colloidal surfaces form an electrical double layer (EDL), which induces electrostatic repulsion between particles. However, the electrostatic repulsion may be weakened in ionic liquids because the thickness of the EDL is less than the molecular size of the ionic liquids, especially when the interparticle distances are long.

Series of experimental evaluation have been done on the dispersion and stability of bare silica nanoparticles in ionic liquids. Results showed that electrostatic repulsion is often not the main reason for the nanoparticles stability in ionic liquids because of the high ionic strength of the ionic liquids. He mentioned several possible stabilization mechanisms of colloidal particles without stabilizers in ionic liquids. In ionic liquid-based steric stabilization, ionic liquid molecules can strongly attach to colloidal surfaces. This attachment may be sufficient to separate colloidal surfaces because many ionic liquids contain nonpolar alkyl groups and polar ionic groups, which can be adsorbed onto either hydrophilic or hydrophobic surfaces. In ionic-based solvation force stabilization, ionic liquid molecules form the multilayered structure around the colloidal particles. This structure can lead to the solvation force, and therefore generate longer-range repulsion. However, ionic liquid-based solvation stabilization can only be used to explain the unusual colloidal stability in certain ionic liquids.

1.3.3 Surface functionalization of nanoparticles

To solve the nanoparticle aggregation problem, based on the study of interaction forces of colloidal particles in medium, researchers focus on steric repulsion stabilization as the common method to improve the stability of nanoparticle dispersion.

In order to achieve steric repulsion to stabilize the colloidal particles, the nanoparticle surface can be functionalized through a tightly bound polymer or a surfactant monolayer [41]. In this approach, adsorbed organic molecules (often polymeric in nature) are utilized to induce steric repulsion. To be effective, the surfactant layer must have an affinity to the solvent so that easy dissolution is enabled. The surfactant layer should be hydrophilic in an aqueous medium and hydrophobic in a low

polar organic medium [42]. Moreover, the adsorbed layers must be of sufficient thickness and density to overcome the Van der Waals attraction between particles and to prevent bridging flocculation [43]. The conformation of adsorbed layers can vary dramatically depending on solvent quality, molecular architecture, number of anchoring groups, active surface site density, as well as colloid and organic concentrations in solution [44]. A schematic illustration of such layers formed by functionalized short-chain dispersants which adsorb on ideal ceramic surfaces are shown in Figure 8. Steric interactions occur when particles approach one another at a separation distance less than twice the adlayer thickness (δ).

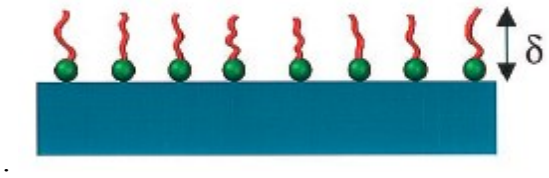

Figure 8. Schematic illustrations of adlayer conformation on an ideal ceramic surface as a function of functional, short-chain dispersant, consisting of anchoring head group and extended tail.

2. EXPERIMENTAL TECHNIQUES AND METHODS *

2.1 Experimental techniques

Various material characterization equipment were used to analyze the characterization of OTS functionalized SiO2 nanoparticles formed in this research project, the tribological and rheological properties of mixtures of nanoparticles (NPs) in ionic liquids (ILs). Specifically, Fourier transform infrared spectroscopy (FTIR), thermal gravimetric analysis (TGA), dynamic light scattering (DLS), Nanotribometry, scanning electron microscopy (SEM) and rheological measurements were used. The following sections will give a brief description of how each equipment works.

2.1.1 Fourier transform infrared spectroscopy (FTIR)

Fourier transform infrared spectroscopy (FTIR) was used to examine the surface of tested substance to provide quantitative and qualitative information in the range from $10cm^{-1}$ to $12{,}800cm^{-1}$. Molecular vibrational states of tested substance are different and the difference in vibrational states may cause adsorption, emission, or reflection of photons. In this method, IR radiation results in the transitions between different molecular vibrational states because IR photons have the same order of magnitude when the energy difference between molecular vibrational states exists. The chemical bonds in the tested substance are identified through the difference between impinging IR radiation and the transmitted radiation [45].

---

* Reprinted with permission form “Inorganic nanoparticle-based ionic liquid lubricant” by Bassem A. Kheireddin, Wei Lu, I-Cheng Chen, Mustafa Akbulut, 2013. Wear, 303, 185-190. Copyright 2013 by Elsevier.

2.1.2 Thermal gravimetric analysis (TGA)

Thermal gravimetric analysis is a method to measurement of sample mass loss according to decomposition, oxidation, or loss of volatiles with the change of temperature, and the mass loss is the function of temperature. In the measurement, the temperature is raised linearly and the sample mass is recorded. At certain temperature, there will be a sharp decrease in mass because of chemical decomposition or boiling. If the boiling or decomposition point of each component in a compound is known, the percentage of different components may be determine by tracking the mass loss with the change of temperature [46].

2.1.3 Dynamic light scattering (DLS)

Dynamic Light Scattering is the measurement of particle size through measuring the random change in the intensity of light scattered from a suspension or solution. In this method, the intensity of light scattered by the molecules in the sample is a function of time. Because all molecules in solution are not stationary and they diffuse in Brownian motion, the diffusion causes interference (constructive or destructive) and results in a change in light intensity. Dynamic Light Scattering can provide information including the average size, size distribution, and polydispersity of molecules and particles in solution according to the measurement of the time scale of light intensity fluctuations.

Moreover, the faster the particles diffuse, the faster the intensity will change. The speed of the intensity change is directly related to the motion of the molecule. The diffusion of the molecules is essentially controlled by the following factors: temperature

(the higher the temperature the faster the molecules will move), viscosity of the solvent (the more viscous the solvent the slower the molecules move) and the size of the molecules (bigger the molecules, the slower they move). Assuming that temperature and solvent are constant, the variation in the intensity of the scattered light is directly related to the size of the molecule. This number is referred to as the hydrodynamic radius (Rh). The hydrodynamic radius is the sphere defined by the molecule rotating in all directions plus the hydration layer. Actually, dynamic Light Scattering is a measurement of how easy it is to move the molecule through the solvent.

2.1.4 Nanotribometry

A nanotribometer is an instrument designed to study the tribological properties between surfaces in contact under dry and lubricated conditions. A large variety of tribometers exist including pin-on-disk, four-ball, block-on-ring, to name a few. In this work, the primary focus will be on a pin-on-disk tribometer the schematic of which is shown in Figure 9. The tribometer used in this study consists of a linear reciprocating module and a cantilever spring assembly. The cantilever spring assembly consists of a spring with a known spring constant at the tip of which a ball holder is located. In addition to the ball holder, two mirrors are located on top of the spring: one mirror is flush with the spring surface and the other perpendicular to it. Each mirror is faced by an optical sensor to allow the detection of normal and lateral deflections. Given the spring constant, and the deflection of the spring, forces can be obtained using Hooke's law.

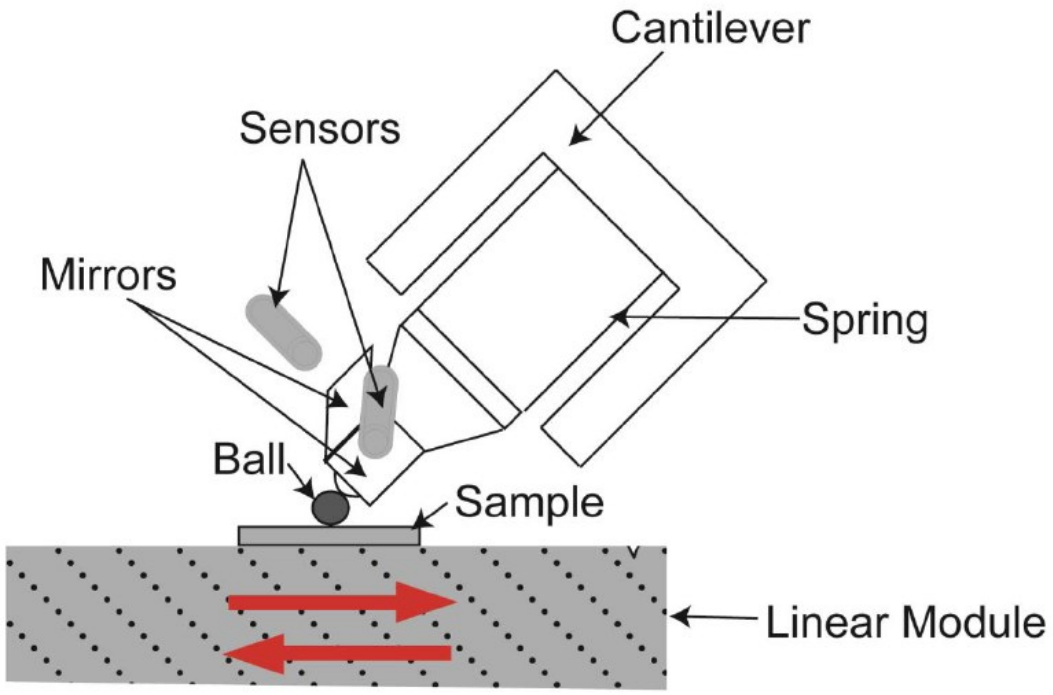

Figure 9. Schematic illustration of the operating principle of a nanotribometer.

2.1.5 Scanning electron microscopy (SEM)

A scanning electron microscope is the measurement of the sample's surface topography and composition by scanning the sample with a focused spot of electrons. The focused spot of electron is about 2-3 nm in diameter. If the resolution of SEM is 2.5 nm, the images can be magnified up to 100,000 times [47]. When the SEM works with the electrons scanning the sample's surface, three types of electrons are released including secondary, backscattered, and transmitted electrons. Backscattered electrons are those that enter the specimen and leave in the direction it came from without

affecting the electrons in the electron shell. Secondary electrons are generated during inelastic collision whereby an electron from the beam knocks out an electron from the inner shell. Because secondary electrons have low energy and have a very slight negative charge, the secondary electrons may be collected by a detector with a positive charge to generate a 3-D image. The brightness of each image pixel is proportional to the electron count in a specific region [48]. There are two requiremwnts for the use of SEM. Firstly, the sample must be stable in high vacuum. In order to realize this condition, the sample has to be dried and fixed or frozen. Secondly, in order to let the sample to reflect enough secondary electron and emit enough secondary back scattered electrons, biological samples need to be coated with a thin layer (~3-4 nm) of conductive material [47].

2.1.6 Rheological properties measurements

Rheological properties measurement can provide more detailed information about the microstructure of the nanoparticles because flow behavior is responsive to properties such molecular weight and molecular weight distribution [49].

Generally, the rheological properties of suspension system can be measured by the rheometer, Most rheometer models belong to three specific categories: rotational, capillary, or extensional. The most commonly used of these is the rotational rheometer, which is also called a stress/strain rheometer, followed by the capillary type.

2.2 Experimental details

2.2.1 Materials

The ionic liquid 1-butyl-3-methylimidazolium (trifluoromethysulfony) imide (BMIM-TSFI) ≥ 98%), and silicon dioxide nanopowder (10-20 nm in size) were purchased from Sigma-Aldrich. Stainless steel sheets with a mirror polish were purchased from Metals Depot (Winchester, KY). Octadecyltrichlorosilane (OTS) was purchased from Gelest Inc. Spectra/Por molecular porous membrane tubing was purchased from Spectrum Laboratories, Inc. All materials were used as received.

2.2.2 Experimental procedures

2.2.2.1 Functionalization of silica nanoparticles

Figure 10 depicts the schematics of the functionalization of SiO2 NPs with OTS, in which surface modification with organosilane moiety generates a core–shell structure [50-52]. The octadecyl group of the OTS (-C18H37) functionalizes the surface of the silica NPs. The functionalization process began with the addition of bare silica nanoparticles to the solution of chloroform and hexane (1:4 in volume). The mixture was then sonicated for 30 minutes to form colloidal suspension. The surfactant OTS was dropped into the mixture and final solution was sonicated for 10 hours to accomplish the coating of the nanoparticles. The unreacted OTS was removed from the mixture by membrane osmosis in chloroform for 8 hours. Finally, the solution was oven dried at room temperature (RT) to obtain the OTS-functionalized nanoparticles.

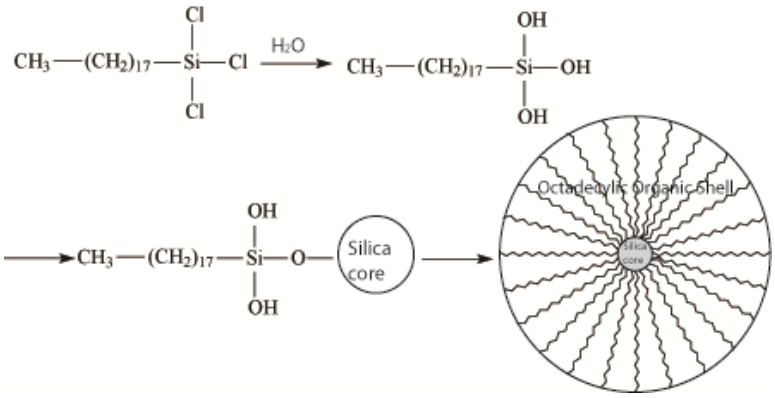

Figure 10. Schematics for the functionalization of SiO2 NPs with OTS.

2.2.2.2 Preparation of silica nanoparticle dispersions in the ionic liquid

The bare silica nanoparticles and the OTS-functionalized nanoparticles were mixed in the hydrophobic ionic liquid-1-butyl-3-methylimidazolium (trifluoromethysulfony) imide. All of the silica nanoparticles dispersions in the ionic liquid were prepared by ultrasonication mixing with a heated digital ultrasonic cleaner (Eumax Instruments, America) for 1 hour to ensure homogeneous mixing.

2.2.2.3 Surface preparation

The steel sheets were cut in the shape of a 2 cm x 2 cm square to form the substrate. Prior to testing, the substrate is cleaned with acetone and blown dry with nitrogen. After testing and shearing the surfaces, the lubricant is removed by rinsing the substrate with acetone, and the substrate is stored for post-shearing characterization.

2.2.3 Analytical methods

2.2.3.1 Characterization of silica nanoparticles

Fourier transform infrared spectroscopy (FTIR) was used to examine the surface modification of silica NPs. The measurements were performed in KBr pellets, containing the samples, under 40 ksi (~275 MPa) pressure via an FT-IR100 spectrometer (Thermo Nicolet).

Thermogravimetric analyses (TGA) were performed via Q500 Thermogravimetric Analyser (TA instruments) to determine the amount of OTS coated on nanoparticle surfaces. The samples were heated between room temperature and 900 °C at a rate of 10°C min^{-1} under N_2 flow.

2.2.3.2 Dynamic light scattering (DLS)

The size distributions of both functionalized and bare SiO_2 NPs in the IL were measured using dynamic light scattering (DLS) (Zetasizer Nano ZS90, Malvern). The first measurement for each sample was made after the samples were sonicated, and second measurement was taken after five minutes. Further measurements were carried out at certain time periods.

2.2.3.3 Friction measurements

The steel sheet samples were cut to form substrates with a dimension of 2cm x 2cm. The substrate was cleaned with acetone and blown dry with nitrogen before testing. Friction response including friction force, friction trace and friction coefficient was undertaken on a nano-tribometer (CSM Instruments, Switzerland) at a constant sliding speed of 0.0005 m/s and a total distance of 0.05 m. All tests were accomplished by

shearing a very smooth stainless steel sphere (diameter ~ 2 mm) with rms roughness of 2.14 ± 0.45 nm on a steel substrate. The smooth stainless steel sphere was lying along a medium-load cantilever with normal and tangential stiffnesses of 150 N/m and 128 N/m, respectively. The normal loads of 5.0, 10.0, 15.0, 20.0, 30.0 and 40.0 mN were applied for each test. For each loading value at least three measurements were taken at several points, and their averages were reported. The maximum coefficient of variance was around 10% for the measurements. In this study, the friction properties of various concentrations of functionalized silica nanoparticles between two steel surface (between stainless steel sphere and steel substrate) were investigated. Throughout this study, the humidity was maintained between 45-50%.

2.2.3.4 Rheological properties measurements

An Anton Paar Rheometer Physica MCR 301(Ashland, VA) with a cone-and-plate geometry (50 mm diameter, 0.987° cone angle) was used for rheological measurements. The gap was set to 0.05 mm throughout the measurements. The shear rate was increased from 1 s^{-1} to 1000 s^{-1} within 10 min allowing and several data points for the viscosity were recorded. The experiments were conducted using Pure IL, and 4 different nanoparticle concentrations (0.05%, 0.1%, 1%, and 5%) dispersed in IL at 22ºC. Each measurement was repeated three times for statistical reliability.

3. RESULTS AND DISCUSSION

3.1 FTIR absorbance of OTS coating on SiO2 NPs

Figure 11 indicates the FTIR spectra of the bare silica NPs, OTS functionalized silica NPs, and pure OTS, as A, B and C, respectively, within the frequency range of 0-4000cm^{-1}. It is clear from the figure that OTS functionalized silica NPs (B) and the pure OTS (C) have significant absorption peaks between 2800-3000cm^{-1}, while the bare silica NPs (A) do not show any peak. Methylene (-CH_2) and methyl (-CH_3) asymmetric and symmetric C-H bands are observed for the molecular structure of pure OTS (C). Methylene (–CH_2) has symmetric and asymmetric stretching at 2850 and 2920 cm-1, respectively, while the methyl (–CH_3) has the same stretching at 2879 and 2968 cm-1, respectively. For the OTS-functionalized silica NPs (B), the CH_2 symmetric and asymmetric stretching was observed at 2851 and 2921 cm^{-1}, respectively, and CH_3 symmetric and asymmetric stretching at 2877 and 2956 cm-1, respectively. The results are in close agreement with the reported data [53-58]. As consequence, the FTIR analysis of the samples indicates that the OTS is coated on the surface of bare silica NPs.

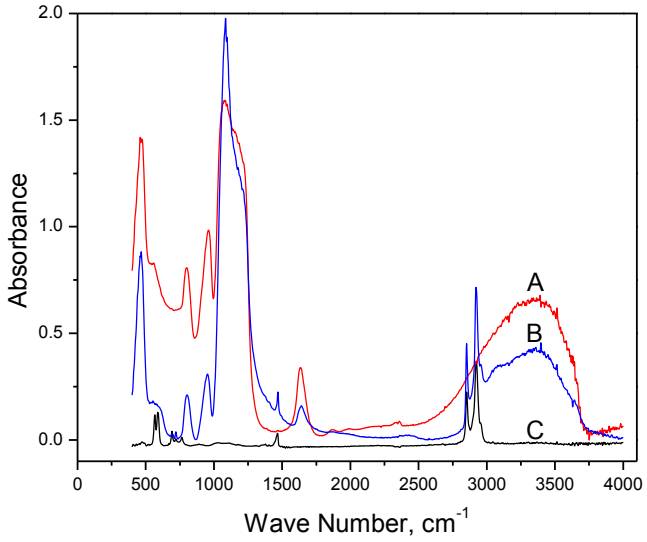

Figure 11. FTIR spectra for (A) bare silica NPs, (B) OTS functionalized silica NPs and (C) pure OTS within the frequency range of 0-4000cm^{-1}.

3.2 TGA behavior of OTS coating on SiO2 NPs

Figure 12 demonstrates the TGA performance of bare and OTS-functionalized SiO_2 NPs. The samples were heated under nitrogen atmosphere from RT to 900°C with a heating rate of 10°C min^{-1}. It is apparent that the weight in both curves decreases around 100°C due to evaporation of water. The small amount of decrease in the OTS-functionalized silica NPs at this temperature compared to the bare silica NPs is due to the hydrophobic nature of OTS-coated sample. The bare silica NPs remain stable for elevated temperatures and do not lose a substantial amount of weight. Meanwhile, the coated SiO_2 NPs sample was stable up to 239°C, which is the main point where the

organic portion (octadecane group: $-C_{18}H_{37}$) of the modified NPs decomposes and the weight decreases drastically. As a result of heating from 239°C up to 900°C, the weight loss of the functionalized silica sample was around 30 wt.%.

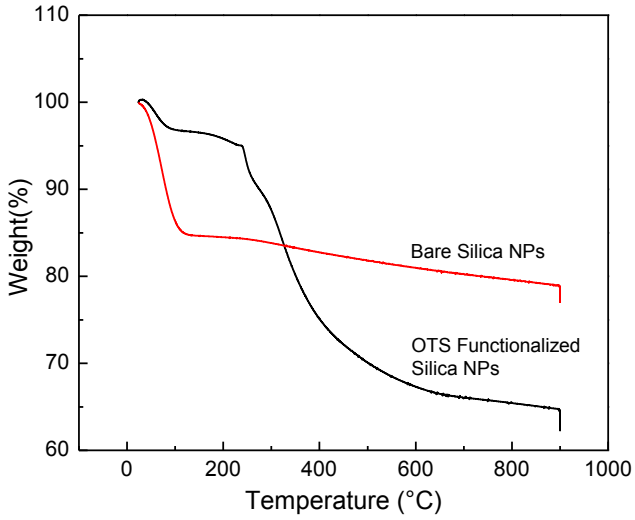

Figure 12. TGA curves between room temperature and 900°C, heating rate of 10°C/min under N_2 atmosphere for bare and OTS-functionalized SiO_2 NPs.

The change in weight of the coated SiO_2 NPs was used to estimate the weight percent of the OTS on the surface of bare SiO_2 NPs. The relationship between specific surface area (SSA) and particle diameter d, can be expressed by Eq. (3) [59]:

$$SSA = \frac{6}{d\rho_{core}} \tag{3}$$

where d is the average diameter of the cores and ρ_{core} is the density of the cores.

For bare SiO_2 NPs, d and ρ_{core} were taken as 20nm and 2.2g/ml, respectively, and the SSA value was determined to be 136.4m^2/g.

The surface density of octadecane group d_O, can be calculated using Eq. (4) [60]:

$$d_O\left(\mu mol/m^2\right) = \frac{\Delta\omega_{shell}/\Delta\omega_{core}}{M_{W,O}SSA} \times 10^6 \tag{4}$$

Where $\Delta\omega_{shell}$ and $\Delta\omega_{core}$ are the percent weight loss for the shell and the core respectively, and $M_{W,O}$, 253g/mol^{-1}, is the molar weight of the octadecane group ($C_{18}H_{37}$). From TGA measurements, $\Delta\omega_{shell}/\Delta\omega_{core}$= 0.3/(0.65) = 0.461. From Eq.(4), the surface density of octadecane group, d_O, was calculated to be approximately 13.37 μmol/m^2.

3.3 Effect of nanoparticle concentration on friction

Eight different concentrations ranging from 0.01 wt.% to 5% were used in this study in order to cover three different concentration regimes: dilute, intermediate and concentrated solutions. As can be seen in Figure 13 and Figure 14, the friction coefficients of bare SiO_2 NPs (A) and OTS functionalized SiO_2 NPs (B) have similar trend, both of them decrease with increasing nanoparticle concentration and then increases gradually. For bare SiO_2 NPs, when the nanoparticle concentration is above 0.05 wt.%, the friction coefficient rises. Therefore, 0.05 wt.% is considered to be the

optimal concentration of bare SiO_2 NPs in the ionic liquid. For OTS functionalized SiO2 NPs, the friction coefficient reaches to a minimum at 0.1 wt.%, it gradually increases with further increase in the concentration. Thus, the optimal concentration of functionalized SiO_2 NPs in the ionic liquid 0.1 wt.%.

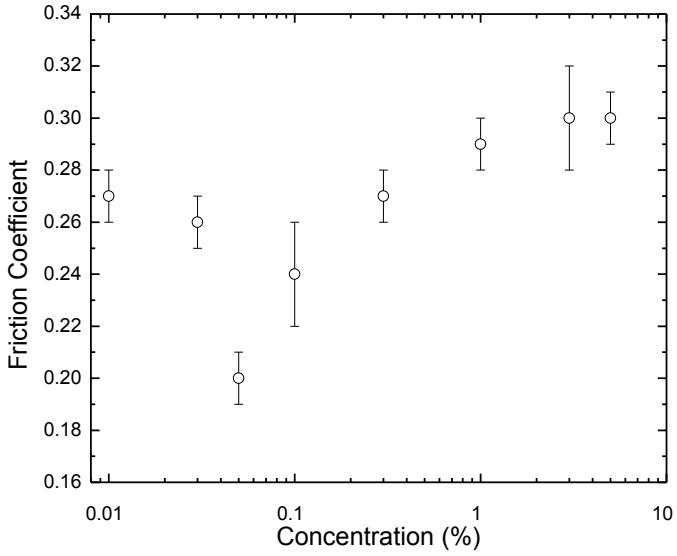

Figure 13. Effect of bare SiO_2 NPs concentration on the friction coefficient.

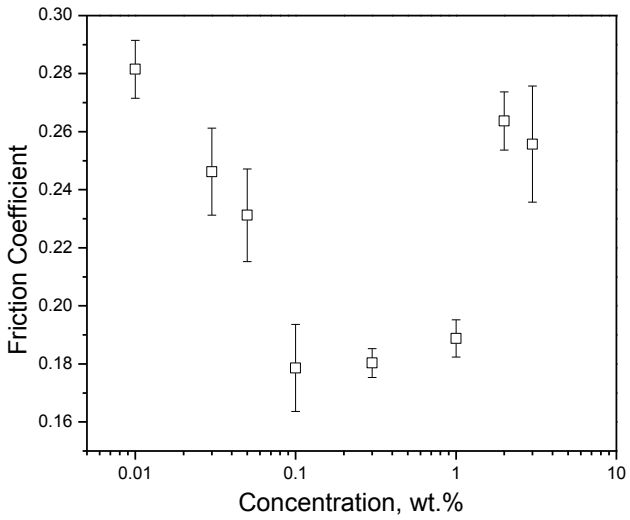

Figure 14. Effect of functionalized SiO_2 NPs concentration on the friction coefficient.

These results can be explained as follows: at very low concentrations, the nanoparticle coverage is low and therefore there are not enough nanoparticles to form a protective film or to prevent contact between asperities, causing the friction coefficient to be relatively high. On the other hand, at high concentrations the nanoparticles tend to form large aggregates and cannot properly fill the valleys between the asperities [61, 62]. Instead, they may behave similar to the debris particles that are known to scratch and wear shearing surfaces under loading and sliding. All of these factors combined suggest that high nanoparticle concentration can have a detrimental effect on the lubrication of shearing surfaces, illustrated by an increase in the friction coefficient [63]. Therefore, it

can be concluded that the optimal concentrations provide enough nanoparticle coverage so that a protective film can be formed without the agglomeration of the nanoparticles.

3.4 Nanoparticle dispersion and colloidal stability

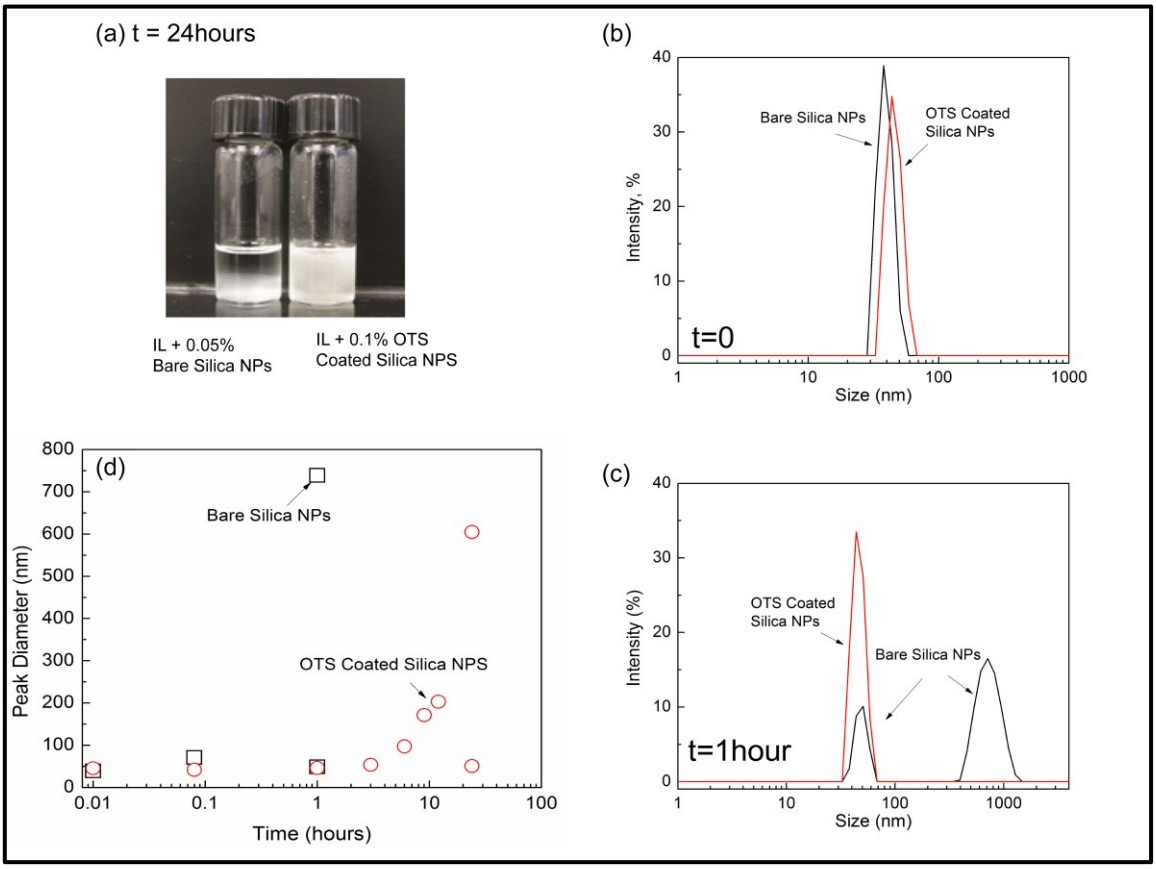

Figure 15. (a) The sedimentation of bare (left) and OTS functionalized SiO_2 NPs in IL (right) after 24 hours from preparation (b) Peak size distribution for bare and OTS functionalized SiO_2 NPs in IL measured by DLS right after sonication (preparation) that was performed to maintain the dispersion of NPs. (c) Peak size distribution for bare and OTS functionalized SiO_2 NPs in IL measured after 1 hour (d) Peak diameter of the bare and OTS functionalized SiO_2 NPs in IL as a function of time.

The photographs of bare and OTS functionalized SiO_2 NPs in IL which were taken after 24 hours from preparation are shown in Figure 15 (a). The former was aggregated and precipitated completely after 24 hours, while the latter seemed to remain stable and a little sedimentation of particles was observed. To elucidate the colloidal stability and NPs dispersion in ILs, size distribution curves of bare and functionalized SiO_2 NPs in IL after immediate preparation (sonication) and after 1 hour are depicted in Figure 4 (b) and (c), respectively. The initial measurement (t=0) shows no significant difference between the peak diameters of uncoated and functionalized NPs. The second measurement which was taken after 1 hour shows that the size distribution of the bare SiO_2 NPs shifts to the right and results in a much larger peak diameter. However, the suspension of the functionalized SiO_2 NPs shows no significant change compared to that of its initial condition. Thus, it can be stated that the functionalized NPs have better colloidal stability in IL than the bare ones. The possible reason is that the surface of the nanoparticles adsorbed around by the organic modification agent can screen out the attractive Van der Waals interactions to prevent the agglomeration [64]. Moreover, further peak size distribution curves of the coated SiO_2 NPs were attained up to 24 hours to show when the bare NPs tend to start aggregation after 1 hour (Figure 4d), the functionalized SiO_2 NPs maintain their colloidal stability in the IL up to 6 hours, and slowly aggregate after that. It can be claimed that they are substantially stable even after 12 hours.

3.5 Effect of nanoparticles on friction

The friction force plot as a function of normal load for the ionic liquid without SiO_2 NPs, IL with 0.05% bare SiO_2 NPs and IL with OTS functionalized 0.1% SiO_2 NPs is shown in Figure 16.

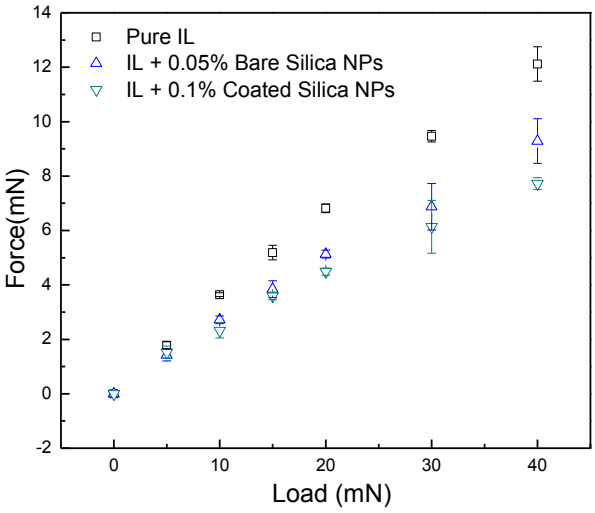

Figure 16. The friction force as a function of load for simply and compositely lubricated conditions.

It is seen that the friction force increases linearly with the normal load for each case, which agrees well with Amontons' law [65]. According the definition of friction

coefficient, the force of friction is directly proportional to the applied load, so the friction coefficient is equal to the proportion of friction force and load, in the figure of friction force and load, the friction coefficient is the slope of every straight line. The friction coefficient of pure IL was determined to be 0.30. Adding bare SiO_2 NPs to the IL reduced the coefficient of friction to 0.23 which is 23% less than that for pure IL, while the addition of functionalized SiO_2 NPs led to a friction coefficient of 0.19 which is 36% less than that for the pure IL. Thus, OTS-coated SiO_2 NPs more effectively decreased the friction coefficient.

It is known that bare SiO_2 NPs dispersed in ILs can adhere to each other and form an aggregate network [66]. This network renders a higher viscosity to the IL and leads to an enhancement of the mechanical properties. Under normal and shear force, the surface valley is filled by the nanoparticles, which results in a better lubrication and a smaller friction coefficient than pure IL. However, the agglomeration of the bare silica nanoparticles damages the colloidal stability of the lubricant suspensions and has a bad effect on their tribological properties [67]. The OTS coating reduces the SiO_2 NPs` tendency to agglomerate and consequently improves the tribological behavior of the ILs.

Furthermore, it was found that at normal loads less than 20mN, the frictional force for the bare and OTS functionalized SiO_2 NPs are almost same, which are lower than those of the pure IL condition. However, at loads above 15mN, the frictional forces of OTS functionalized SiO_2 NPs in the IL becomes less than those of bare SiO_2 NPs. This is due to the faster sedimentation of bare silica NPs during friction force measurement process than the OTS coated silica NPs.

3.6 Rheological properties

The rheology experiments of the pure IL and various concentrations of bare SiO_2 and OTS functionalized SiO_2 dispersions were conducted to determine the viscosity of NPs suspension, as shown in Figure 17a and 17b, respectively.

Both figures indicate that the viscosity increases as the concentration of SiO_2 NPs increases, which is consistent with that reported in previous studies dealing with SiO_2 dispersions in ionic liquids and similar systems [66, 68-70]. This was an expected result, because an increase in the NPs concentration enhances the possibility of nanoparticle agglomeration and eventually leads to the gelation of the ionic liquid. Also, the results obtained in this study agree well with those reported elsewhere [66, 71]. Moreover, a Newtonian fluid behavior is seen in the pure IL, 0.05 wt.%, and 0.1 wt.% NP dispersion where the viscosity is independent of the shear rate. However, the viscosity is dependent on the shear rate at higher concentrations, which agrees with the previous studies. This indicates that agglomerates and networks tend to occur at low shear rates, when the concentration is high, and that network structure is destructed by increasing the shear rate [69]. Therefore, at concentrations above the optimal value the nanoparticle suspension is claimed to be unstable.

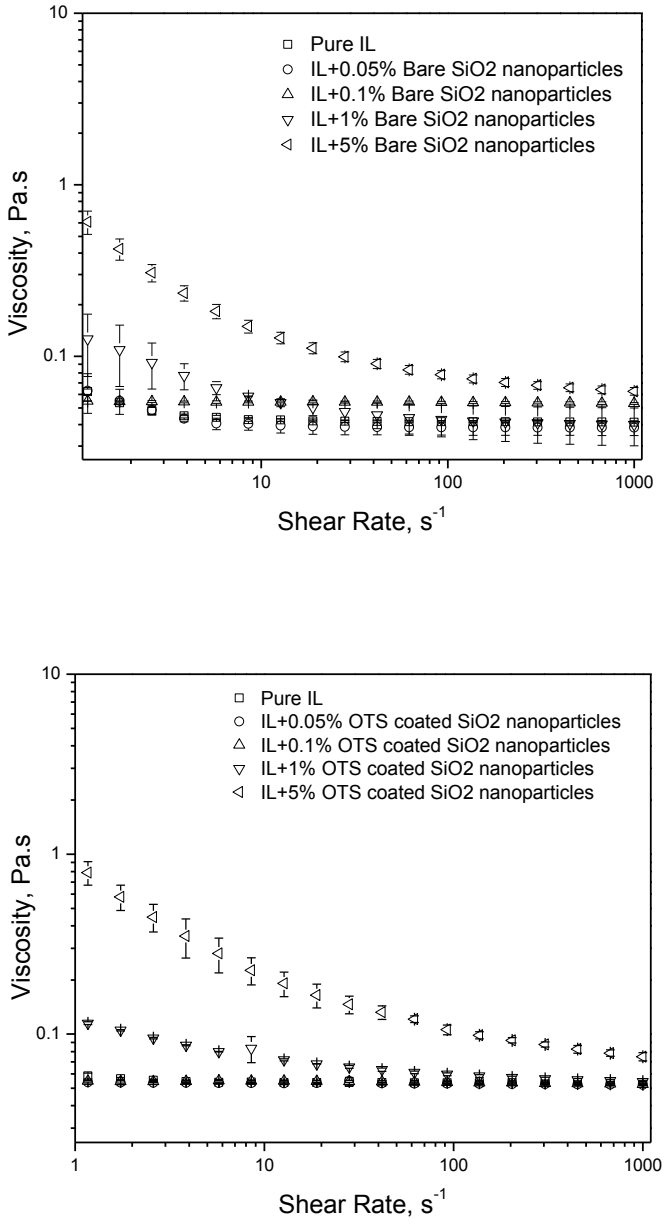

Figure 17. Viscosity of the neat IL and IL with various concentrations of (a) SiO_2 NPs and (b) OTS Coated (Functionalized) SiO_2 NPs as a function of shear rate.

3.7 Wear behavior of surfaces

The scanning electron microscope (SEM) was employed to investigate the worn surface of pure IL and compositely lubricated conditions (0.05wt% bare SiO_2 NPs+IL and 0.1wt% OTS functionalized SiO_2 NPs+IL) at a 20mN load. The photos are shown in Figure 18.

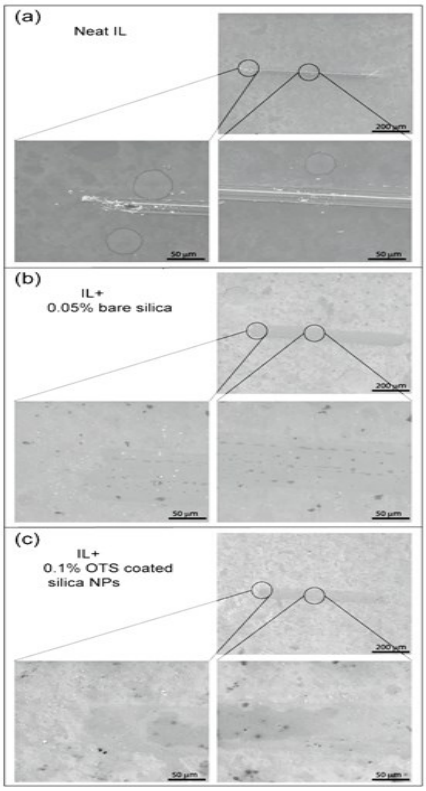

Figure 18. SEM morphologies of steel surfaces after shearing under three different lubrication conditions: (a) neat IL (b) IL+ 0.05 wt.% bare SiO_2 NPs and (c) IL + 0.1 wt.% OTS functionalized SiO_2 NPs. Low and high magnifications of the middle and edge parts of the wear track are shown.

As shown in Figure 18(a), large debris is observed on the worn surface of steel under pure ionic liquid. Contrary to (a), the worn surfaces of steel in Figure 18b and 18c are smoother that that under pure ionic liquid. Also, the NPs are deposited on the worn surface and the tribological behaviors of them as ionic liquid additive improved significantly as compared with that of pure ionic liquid. This implies that under a 20mN load, the deposition of NPs on the worn surface can decrease the shearing stress, and hence reduce friction and wear.

3.8 Friction traces

Detailed information about dynamics of lubricant under load and shearing can be observed by the analysis of friction trace. Figure 19 shows the friction traces for the initial and steady state sliding for pure IL, IL+0.05% bare SiO_2 NPs and IL+ 0.1% OTS funcionalized SiO_2 NPs.

For ionic liquid without NPs, evident stick-slip spikes were observed in steady state compared to the initial state. Moreover, the steady state friction force increased around 5.8% than that of the initial one due to increase in wear volume with sliding distance. This result is in accordance with the SEM images of the worn surface in Figure18(a), where a heavy damage occurs under the pure IL condition. When 0.05% bare SiO_2 NPs were added to the IL, the steady state friction force decreased about 18.7% compared to the initial one. Also, the amplitude of the stick-slip is significantly lower than that of the pure IL condition. On the other hand, the addition of 0.1% OTS functionalized SiO_2 NPs to the IL made the movement steady and the stick-slip spikes almost disappeared.

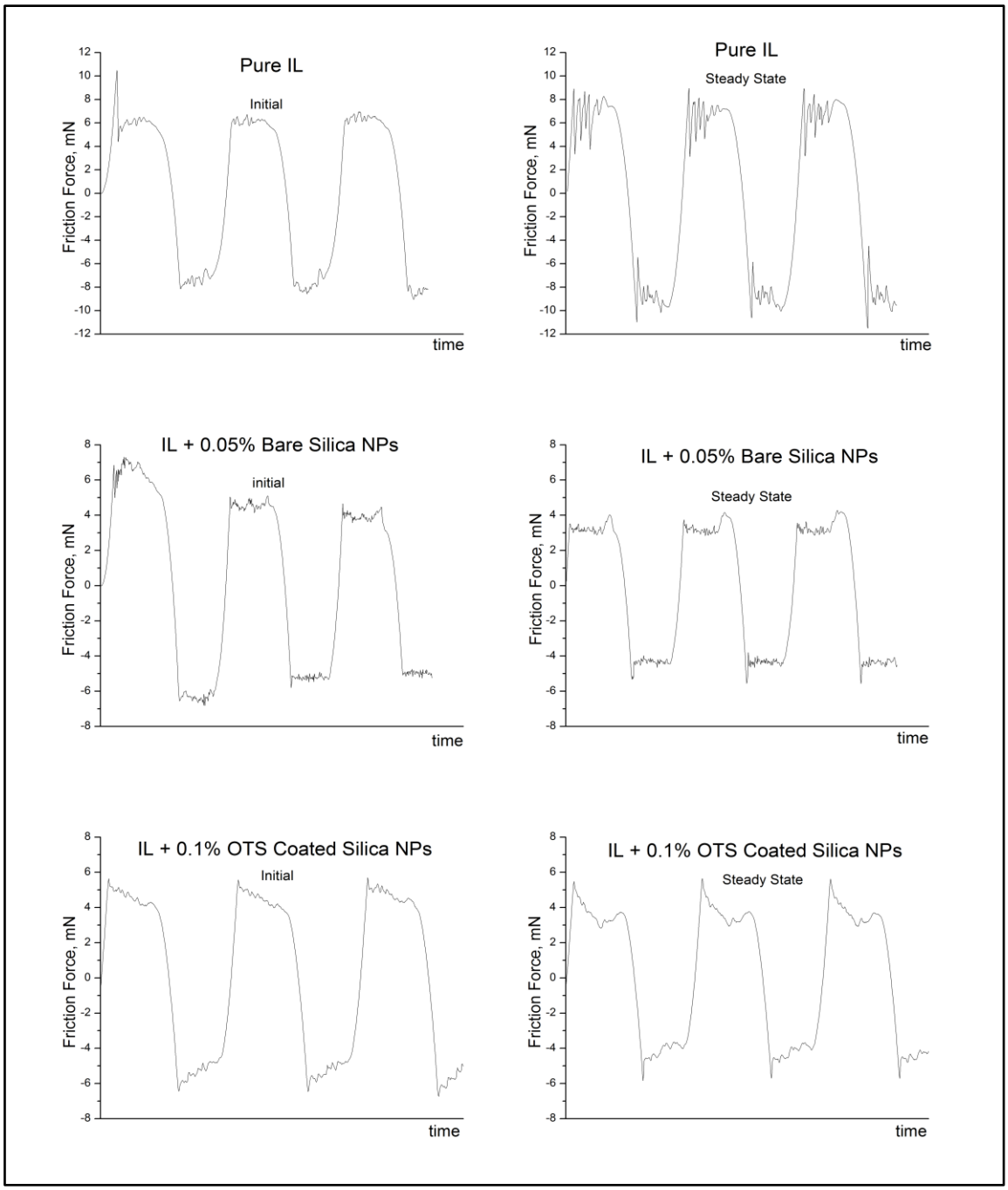

Figure 19. Initial and steady-state friction traces for pure IL, IL + 0.05 wt.% bare SiO_2 NPs and IL + 0.1 wt.% OTS functionalized SiO_2 NPs which were obtained for 20mN load. They are drawn to scale.

The steady state friction force was about 23.4% less than that of the initial one. Since high amplitudes of stick-slip spikes are associated with severe damage and low amplitudes mean minimal damage, it can be concluded that the OTS functionalized SiO_2 NPs in IL considerably reduce the stick-slip spikes, raise the stability of motion and provide a better lubrication performance than bare SiO_2 NPs.

4. CONCLUSION

In summary, this thesis presents the tribological properties of two nanoparticle-based lubrication systems-bare SiO2 NPs and Hydrophobic monolayer-octadecyltrichlorosilane (OTS) functionalized SiO2 NPs dispersed in ionic liquid, 1-butyl-3-methylimidazolium (trifluoromethy-sulfony) imide. The tribological properties of various concentrations of bare and OTS functionalized SiO_2 NPs in the ionic liquid were investigated and shown that: (1) the hydrophobic monolayer of octadecyltrichlorosilane (OTS) was coated on the surface of bare SiO_2 nanoparticles and the surface density of octadecane group was estimated to be 13.4μmol/m^2. (2) The dispersion of the OTS functionalized SiO_2 NPs in the ionic liquid could have better colloidal stability compared to bare SiO_2 NPs dispersed in the same ionic liquid according to DLS tests. (3) At the optimal concentration, the OTS functionalized SiO_2 NPs dispersed in the ionic liquid show tribological properties which are superior to the pure ionic liquid and bare SiO_2 NPs in the ionic liquid in terms of providing the best friction-reduction and anti-wear properties for steel/steel contact.

As for future prospective, the characterization and applications of various hydrophobic monolayer modified SiO_2 NPs dispersed green solvents such as ionic liquids are encouraged.

REFERENCES

1. Rabinowicz, E., *Friction and wear of materials.* New York: Wiley, 2005.
2. Jost, H. P., *Tribology: how a word was coined 40 years ago.* Tribology & Lubrication Technology, 2006. **62**: p. 24-28.
3. Dowson, D., *History of tribology,* 2nd ed., Professional Engineering Publishing: London, UK, 1998. p. 23-42.
4. Zhou, F., Liang, Y., and Liu, W., *Ionic liquid lubricants: designed chemistry for engineering application.* Chemical Society Reviews, 2009. **38**: p. 2590-2599.
5. Maria F., Wayne C. N., Patrick C. H., Douglas R. M., *New insights into the fundamental chemical nature of ionic liquid film formation on magnesium alloy surfaces.* ACS Applied Materials and Interfaces, 2009. **1(5)**: p. 1045–1052.
6. Hamrock, B. J., Schmid, S. R., and Jacobson, B. O., *Fundamentals of fluid film lubrication,* CRC, 2nd ed, 2004.
7. Bermudez, M. D., Jimenez, A. E., Sanes, J. and Carrion, F. J., *Ionic liquids as advanced lubricant fluids.* Molecules, 2009. **14**: p. 2888-2980.
8. Pensado, A. S., Comunas, M. J. P., and Fernandez, J., *The pressure–viscosity coefficient of several ionic liquids.* Tribology Letters, 2008. **31**: p. 107-118.
9. Wilkes, J. S., Leviski, J. A., Wilson, R. A., Hussey, C. L., *Dialkylimidazolium chloroaluminate melts: a new class of room-temperature ionic liquids for electrochemistry, spectroscopy and synthesis*. Inorganic Chemistry, 1982. **21**: p. 1263-1264.

10. Wilkes, J. S., Zaworotko, M. J., *Air and water stable 1-ethyl-3-methylimidazolium based ionic liquids.* Chemical Community, 1992. p. 965-967.

11. Ye, C. F., Liu, W. M., Chen, Y. X., Yu, L. G., *Room-temperature ionic liquids: a novel versatile lubricant.* Chemical Community, 2001. p. 2244-2245.

12. Zhou, F., Liang, Y., and Liu, W., *Ionic Liquid Lubricants: Designed chemistry for engineering application.* Chemical Society Reviews, 2009. **38**: p. 2590-2599.

13. Suzuki, A., Shinka, Y., Masuko, M., *Tribological characteristics of imidazolium-based room temperature ionic liquids under high vacuum.* Tribology Letters, 2007. **27**: p. 307-313.

14. Phillips, B. S. and Zabinski, J. S. *Ionic liquid lubrication effects on ceramics in a water environment*. Tribology Letters, 2004. **17**: p. 533-541.

15. Omotowa, B. A., Phillips, B. S., Zabinski, J. S., Shreeve, J. M., *Phosphazene-based ionic liquids: Synthesis, temperature-dependent viscosity, and effect as additives in water lubrication of silicon nitride ceramics.* Inorganic Chemistry, 2004. **43**: p. 5466-5471.

16. Jimenez, A. E., Bermudez, M. D., Carrion, F. J., Martinez-Nicolas, G., *Room temperature ionic liquids as lubricant additives in steel-aluminium contacts: influence of sliding velocity, normal load and temperature.* Wear, 2006. **261**: p. 347-359.

17. Jimenez, A. E., Bermudez, M. D., *Imidazolium ionic liquids as additives of the synthetic ester propylene glycol dioleate in aluminium-steel lubrication.* Wear, 2008. **265**: p. 787-798.

18. Yao, M., Liang, Y., Xia, Y., Zhou, F., *Bisimidazolium ionic liquids as the high-performance antiwear additives in poly(ethylene glycol) for steel−steel contacts.* ACS Applied Materials & Interfaces, 2009. **1**: p. 467-471.

19. Forsyth, M., Kemp, T. F., Howlett, P. C. et al, *A potential novel rapid screening NMR approach to boundary film formation at solid interfaces in contact with ionic liquids.* The Journal of Physical Chemistry, 2008. **112**: p. 13801-13804.

20. Nooruddin, N. S., Wahlbeck, P. G., and Carper, W. R., *Semi-empirical molecular modeling of ionic liquid tribology: ionic liquid–hydroxylateds silicon surface interactions.* Tribology Letters, 2009. **36**: p. 147–156.

21. Kajdas, C., *Importance of anionic reactive intermediates for lubricant component reactions with friction surfaces.* Lubrication Science, 1994. **6**: p. 203.

22. Li, B., Wang, W., Liu, W., Xue, Q., *Tribochemistry and antiwear mechanism of organic-inorganic nanoparticles as lubricant additives.* Tribology Letters, 2006. **22**(1): p. 79-85.

23. Akbulut, M., et al., *Frictional properties of confined nanorods.* Advanced Materials, 2006. **18**(19): p. 2589-2592.

24. Rapoport, L., Fleischer, N., and Tenne, R., *Fullerene-like WS2 nanoparticles: superior lubricants for harsh conditions.* Advanced Materials, 2003. **15**(7-8): p. 651-655.

25. Dickrell, P. L., et al., *Tunable friction behavior of oriented carbon nanotube films.* Tribology Letters, 2006. **24**(1): p. 85-90.

26. Enomoto, K., et al., *Frictional properties of carbon nanofiber reinforced polymer matrix composites.* New Diamond and Frontier Carbon Technology, 2004. **14**(1): p. 11-20.

27. Chen, W. X., et al., *Tribological application of carbon nanotubes in a metal-based composite coating and composites.* Carbon, 2003. **41**(2): p. 215-222.

28. Cumings, J. and Zettl, A., *Low-friction nanoscale linear bearing realized from multiwall carbon nanotubes.* Science, 2000. **289**(5479): p. 602-604.

29. Falvo, M. R., et al., *Nanometre-scale rolling and sliding of carbon nanotubes.* Nature, 1999. **397**(6716): p. 236-238.

30. Pawlak, Z., et al., *The tribochemical and micellar aspects of cutting fluids.* Tribology International, 2005. **38**: p. 1-4.

31. Peng, D. X., Kang, Y., et al., *Tribological properties of diamond and SiO2 nanoparticles added in paraffin.* Tribology International, 2009. **42**: p. 911-917.

32. Bessem A. K. (2013). *Tribological properties of nanoparticle-based lubrication systems.* Ph.D. Dissertation, Texas A&M University (College Station, TX).

33. Martin, J. M. and Ohmae, N., *Nanolubricants.* Chichester: Wiley, 2008.

34. Rapoport, L., et al., *Tribological properties of WS2 nanoparticles under mixed lubrication.* Wear, 2003. **255**(7–12): p. 785-793.

35. Chen, S., Liu, W., and Yu, L., *Preparation of DDP-coated PbS nanoparticles and investigation of the antiwear ability of the prepared nanoparticles as additive in liquid paraffin.* Wear, 1998. **218**(2): p. 153-158.

36. Liu, W. and Chen, S., *An investigation of the tribological behaviour of surface-modified ZnS nanoparticles in liquid paraffin.* Wear, 2000. **238**(2): p. 120-124.

37. Li, B., Wang, W., Liu, Xue, Q., *Tribochemistry and antiwear mechanism of organic-inorganic nanoparticles as lubricant additives.* Tribology Letters, 2006. **22** (1): p. 79-85.

38. Ueno, K., Imaizumi, S. et al., *From colloidal stability in ionic liquids to advanced soft materials using unique media.* Langmuir, 2011. **27**: p. 9105-9115.

39. Lewis, J. A., *Colloidal processing of ceramics*. Journal of the American Ceramic Society, 2000. **83**(10): p. 2341–2359.

40. Hayes, R., Warr, G., Atkin, R., *At the interface: solvation and designing ionic liquids.* Physical Chemistry Chemical Physics, 2010. **12**: p. 1709.

41. Min, Y. J., et al., *The role of interparticle and external forces in nanoparticle assembly.* Nature Materials, 2008. **7**(7): p. 527-538.

42. Bakunin, V. N., et al., *Synthesis and application of inorganic nanoparticles as lubricant components - a review.* Journal of Nanoparticle Research, 2004. **6**(2-3): p. 273-284.

43. McClements, D. J., *Theoretical analysis of factors affecting the formation and stability of multilayered colloidal dispersions.* Langmuir, 2005. **21**(21): p. 9777–9785.

44. Napper, D. H., *Polymeric stabilization of colloidal dispersions*. Academic Press, London, U.K., 1983. p. 4–13.

45. Nyquist, R. A. and Putzig, C. L., *Infrared spectroscopy, encyclopedia of analytical science.* Ed. A. Townshend, San Diego: Academic Press, 1995. **4**: p. 2153-2170.

46. Hill, J. O., *Thermogravimetry*, Encyclopedia of Analytical Science, Ed. A. Townshend, San Diego: Academic Press, 1995. **8**: p. 5141-5143.

47. Hoppert, M., *Microscopic techniques in biotechnology*. 1st ed., Weinheim: Wiley, 2003. p.147-192.

48. Bozzola, J., and Russell, L., *Electronm microscopy: principles and techniques for biologists.* Sudbury: Jones and Bartlett Publishers, 1999. p.17-208.

49. Wang, B., Wang, X., Lou, W. and Hao, J., *Rheological and tribological properties of ionic liquid-based nanofluids containing functionalized multi-walled carbon nanotubes.* Journal of Physical Chemistry C, 2010. **114**: p. 8749-8754.

50. Rahmana, I. A., Vejayakumaran, P., Sipaut, C. S., Ismail, J., *An optimized sol–gel synthesis of stable primary equivalent silica particles.* Colloids and Surfaces A: Physicochemical Engineering Aspects, 2007. **294**: p. 102-110.

51. Marini, M., Pourabbas, B., Pilati, F., Fabbri, P. *Functionally modified core-shell silica nanoparticles by one-pot synthesis.* Colloids and Surfaces A: Physicochemical Engineering Aspects, 2008. **317**: p. 473-481.

52. Bourlinos, A. B., Herrera, R., Chalkias, N., Jiang, D., Zhang, Q., Archer, L. A., Giannelis E. P. *Surface-functionalized nanoparticles with liquid-like behavior*. Advanced Materials, 2005. **17**: p. 234-237.

53. Brandriss, S., Margel, S., *Synthesis and characterization of self-assembled hydrophobic monolayer coatings on silica colloids*. Langmuir, 1993. **9**: p. 1232-1240.

54. Maoz, R., Sagiv, J., *On the formation and structure of self-assembling monolayers. I. A comparative air-wettability study of Langmuir—Blodgett and adsorbed films on flat substrates and glass microbeads*. Colloid and Interface Science, 1984. **100**(2): p. 465–496.

55. Margel, S., Sivan, O., Dolitzky, Y., *Functionalized thin films: synthesis, characterization, and potential use.* Langmuir, 1991. **7**: p. 2317.

56. Mirji, S. A. *Octadecyltrichlorosilane adsorption kinetics on Si(100)/SiO2 surface: contact angle, AFM, FTIR and XPS analysis.* Surface and Interface Analysis, 2006. **38**: p.158–165.

57. Jeon, N. L., Finnie, K., Branshaw, K., Nuzzo, R. G., *Structure and stability of patterned self-assembled films of octadecyltrichlorosilane formed by contact printing.* Langmuir, 1997. **13**: p. 3382-3391.

58. Hoffmann, H., Mayer, U., Krischanitz, A., *Structure of alkylsiloxane monolayers on silicon surfaces investigated by external reflection infrared spectroscopy.* Langmuir, 1995. **11**(4): p. 1304-1312.

59. Rahmana, I. A., Vejayakumaran, P., Sipaut, C. S., Ismail, J., *An optimized sol–gel synthesis of stable primary equivalent silica particles*. Colloids and Surfaces A: Physicochemical and Engineering Aspects, 2007. **294**: p. 102-110.

60. Marini, M., Pourabbas, B., Pilati, F., Fabbri, P., *Functionally modified core-shell silica nanoparticles by one-pot synthesis.* Colloids and Surfaces A: Physicochemical Engineering Aspects, 2008. **317**: p. 473-481.

61. Moshkovith, A., Perfiliev, V., Lapsker, I., Fleischer, N., *Friction of fullerene-like WS2 nanoparticles: effect of agglomeration.* Tribology Letters, 2006. **24**: p. 225-228.

62. Rapoport, L., Fleischer, N., Tenne, R., *Fullerene-like WS2 nanoparticles: superior lubricants for harsh conditions.* Advanced Materials, 2003. **15**: p. 651-655.

63. Bartz, W.J., *Solid lubricant additives - effect of concentration and other additives on anti-wear performance.* Wear, 1971. **17**: p. 421-432.

64. Peng, D. X., Chen, C. H., Kang, Y., Chang, Y. P., Chang S. Y., *Size effects of SiO2 nanoparticles as oil additives on tribology of lubricant*. Industrial Lubrication and Tribology, 2010. **62**: p.111-120.

65. Gao, J., Luedtke, W. D., Gourdon, D., Ruths, M., Israelachvili, J. N., Landman, U., *Frictional Forces and Amontons' Law: From the molecular to the macroscopic scale.* The Journal of Physical Chemistry B, 2004. **108**: p. 3410-3425.

66. Kheireddin, B., Lu, W., Chen, I., Akbulut, M., *Inorganic nanoparticle-based ionic liquid lubricants.* Wear, 2013. **303**: p. 185-190.

67. Shahar, C., Zbaida, D., Rapoport, L., Cohen, H., Bendikov, T., Tannous, J., Dassenoy, F., Tenne, R., *Surface functionalization of WS2 fullerene-like nanoparticles*. Langmuir, 2010. **26**: p. 4409-4414.

68. Ueno, K., Imaizumi, S., Hata, K., Watanabe, M., *Colloidal interaction in ionic liquids: effects of ionic structures and surface chemistry on rheology of silica colloidal dispersions.* Langmuir, 2008. **25**: p. 825-831.

69. Wittmar, A., Ruiz-Abad, D., Ulbricht, M., *Dispersions of silica nanoparticles in ionic liquids investigated with advanced rheology.* Journal of Nanoparticle Research, 2012. **14**(651): p. 1-10.

70. Wang, B., Wang, X., Lou, W., Hao, J., *Rheological and tribological properties of ionic liquid-based nanofluids containing functionalized multi-walled carbon nanotubes.* The Journal of Physical Chemistry C, 2010. **114**: p. 8749-8754.

71. Chen, H., He, Y., Zhu, J., *Rheological and heat transfer behaviour of the ionic liquid, [C_4mim][NTf_2]*. Internal Journal of Heat and Fluid Flow, 2008. **29**: p.149-155.